Hindawi
Mathematical Problems in Engineering
Volume 2017, Article ID 7835049, 9 pages
https://doi.org/10.1155/2017/7835049

Research Article

Capacity Fast Prediction and Residual Useful Life Estimation of Valve Regulated Lead Acid Battery

Qin He,[1,2] Yabing Zha,[1] Quan Sun,[1] Zhengqiang Pan,[1] and Tianyu Liu[1]

[1] *College of Information System and Management, National University of Defense Technology, Changsha 410073, China*
[2] *School of Mechanical and Electrical Engineering, Shandong Jianzhu University, Jinan 250000, China*

Correspondence should be addressed to Tianyu Liu; liutianyu@nudt.edu.cn

Received 14 June 2016; Accepted 27 December 2016; Published 20 February 2017

Academic Editor: Dane Quinn

The usable capacity of acid lead batteries is often used as the degradation feature for online RUL (residual useful life) estimation. In engineering applications, the "standard" fully discharging method for capacity measure is quite time-consuming and harmful for the high-capacity batteries. In this paper, a data-driven framework providing capacity fast prediction and RUL estimation for high-capacity VRLA (valve regulated lead acid) batteries is presented. These batteries are used as backup power sources on the ships. The relationship between fully discharging time and partially discharging voltage curve is established for usable capacity extrapolation. Based on the predicted capacity, the particle filtering approach is utilized to obtain battery RUL distribution. A case study is conducted with the experimental data of GFM-200 battery. Results confirm that our method not only reduces the prediction time greatly but also performs quite well in prediction accuracy of battery capacity and RUL.

1. Introduction

VRLA (valve regulated lead acid) batteries are widely used in ships, electric vehicles, uninterruptible power supply, and mobile communication facilities, given that they have outstanding properties of high capacity, good stability, low cost, and easy recovery [1]. During operation, a series of electrochemical and physical side reactions occur in the battery, which lead to permanent degradation of battery capacity, internal resistance, power density, and other performance characteristics [2]. The EOL (end-of-life) of a VRLA battery is defined as the moment at which these above performance characteristics cannot meet the requirements [3]. Cycle life is one of the important indexes to measure battery performance and quality, which is generally denoted by the total number of charge/discharge cycles that a new battery experiences before reaching the EOL. In practice, users and engineers are more concerned about the RUL of batteries, namely, the remaining charge/discharge cycle a battery has from the present to the EOL. An accurate RUL estimation model can adequately provide scientific and reasonable basis for strategies of battery maintenance and replacement. And it is also the key technique of the battery management system (BMS).

Capacity fading is the main failure mode of VRLA batteries. And the continuous capacity loss is due to calendar storage and cyclic charge-discharge. According to the corresponding industrial standard, a VRLA battery fails when the usable capacity fades to 70%~80% of its initial amount. Therefore, the accurate measurement of usable capacity is the premise to perform RUL estimation of VRLA batteries. Conventionally, the capacity of a VRLA battery can be accurately measured by the fully discharging method, in which a full charge/discharge cycle is conducted and the amount of electricity that the battery releases is recorded. However, the method cannot be directly applied on the high-capacity VRLA directly [4]. Generally, a fully discharging process of the high-capacity VRLA battery lasts at least ten hours. Although the measure time can be shortened by a large current, it would lead to incomplete discharge and then underestimation of capacity compared to the actual value and even cause permanent damage to the VRLA battery and seriously shorten its cycle life [4]. Furthermore, the discharging process for a battery stack, which is composed of

a large number of serial battery cells, has to stop, once any one of cells is fully discharged. In other words, the cell with the lowest capacity limits the capacity measurement of other cells [5]. Therefore, the fully discharging method does not work on the battery stack which comprises a variety of serial cells.

The work in this paper is motivated by a practical engineering problem of backup VRLA batteries on the ships. In ordinary days, it is the diesel engine generator that supplies power for the electric loadings. And the batteries are stored in the float mode as standby. Only in the emergency when the diesel engine stops work due to some accidents are the VRLA batteries activated and begin to provide power for some especially important loadings, like the communication equipment, light facilities, and so forth. To ensure that the batteries can supply enough energies (or capacity) in the emergency, engineers need to measure the maximum discharge capacity regularly (e.g., every three months). As discussed above, the traditional fully discharging method is quite time-consuming and shortens battery life seriously owing to the deep discharge. To this end, we aim at developing a fast capacity prediction approach to help check the health status of backup batteries periodically and then estimate their residual cycle life.

In our paper, we focus on the capacity prediction and RUL estimation of high-capacity VRLA batteries used as backup power on the ships. A lot of experiments reveal that the discharge voltage curve of a VRLA battery regularly varies with the battery aging [6]. Thus, it can be applied to predict the usable capacity. In consideration of the feature, a novel capacity fast prediction method based on the partially discharging voltage curve is developed. Through discharging a fully charged battery in a relatively short period of time, the voltage variation is used to estimate the parameters of the discharge voltage model and then to extrapolate the fully discharging time and usable capacity. Under the framework of particle filtering, the capacity prediction results are used as the degradation feature to perform the online RUL estimation. A case study with respect to GFM-200 valve regulated lead acid battery demonstrates the effectiveness of our method in both the accuracy of usable capacity prediction and RUL estimation.

2. Characteristics of VRLA Batteries

2.1. A Brief Introduction to VRLA Batteries. VRLA batteries have the merit of no leakage of acid or acid mist due to their rigorously sealed structure. In operation, it is not necessary to replenish acid or water to ensure that VRLA batteries work constantly. A safety valve is installed on the battery jar. Once the pressure inside the battery increases to a certain level, the valve automatically opens to release extrato release gas and then shuts down to keep the outside air from entering. During the charge/discharge process, the chemical reactions on the positive and negative electrodes of VRLA batteries are reversible. The active material of the anode is lead dioxide and the main constituent of the cathode is cavernous lead. The electrolyte is dilute sulfuric acid. The main reactions of VRLA battery during the charge and discharge process are shown as follows:

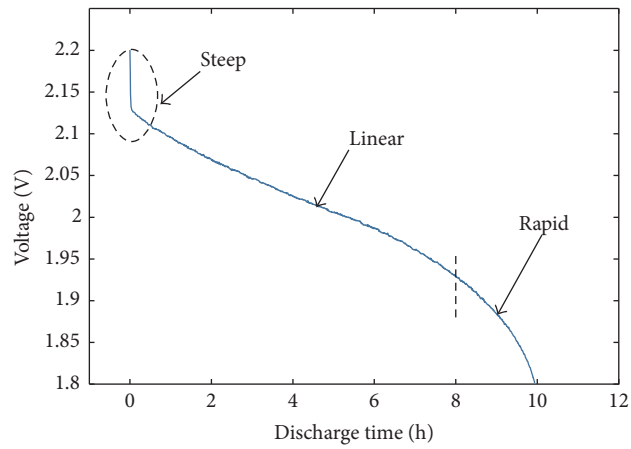

Figure 1: Battery discharge voltage in one cycle.

(i) Charge

Anode

$$PbSO_4 + 2H_2O \longrightarrow PbO_2 + H_2SO_4 + 2H^+ + 2e^- \quad (1)$$

Cathode

$$PbSO_4 + 2H^+ + 2e^- \longrightarrow Pb + H_2SO_4 \quad (2)$$

(ii) Discharge

Anode

$$PbO_2 + H_2SO_4 + 2H^+ + 2e^- \longrightarrow PbSO_4 + 2H_2O \quad (3)$$

Cathode

$$Pb + H_2SO_4 \longrightarrow PbSO_4 + 2H^+ + 2e^- \quad (4)$$

The terminal voltage of lead acid battery depends on the electrolyte concentration. In the discharge, battery voltage drops gradually as the electrolyte concentration decreases, while it rises in the charge as the electrolyte concentration increases [6].

VRLA batteries work in a wide range of temperature. The rated voltage of a single VRLA battery is usually 2 V, the discharge cut-off voltage is 1.75–1.8 V, and the charge cut-off voltage is 2.35 V. The charge regime could be constant current and constant voltage (CC-CV) charge or constant voltage (CV) floating charge. For the high-capacity VRLA batteries, the current in the fully discharging method should be less than 0.1 C in order to protect it from shocks and damage. For a 200 Ah battery, 0.1 C represents a current of $200 \times 0.1 = 20$ A.

2.2. Discharge Characteristics. Figure 1 shows the voltage curve of a fully charged lead acid battery during the constant current discharge. It is clear that the voltage curve of discharge can be divided into three phases. In the first phase, battery voltage experiences a steep drop in a short period

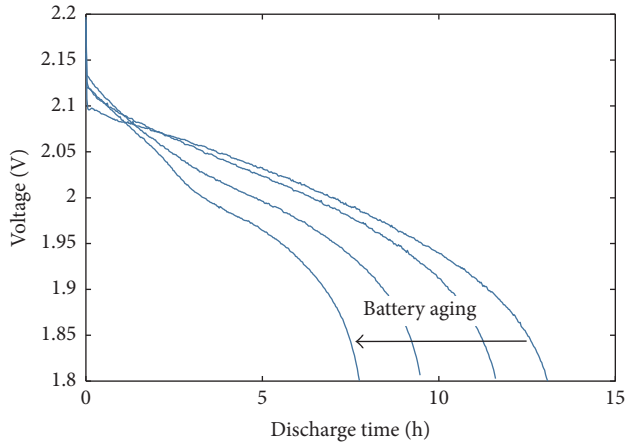

Figure 2: Battery discharge voltage in different cycles.

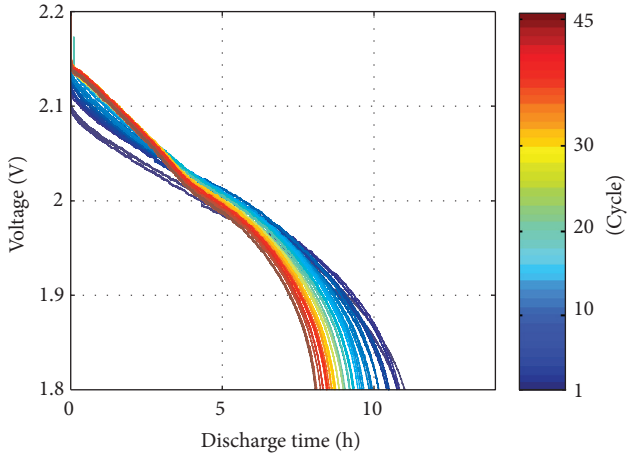

Figure 3: Testing results of GFM-200 battery.

of time (about 5 minutes), which is caused by the internal resistance of the battery. A VRLA battery normally works in the second phase. During this period, the electrochemical reactions inside the battery tend to be stable, and the voltage shows an approximately linear decrease over time. In the last phase, the voltage drops rapidly to the cut-off voltage. Figure 2 shows the variation of discharge voltage curves in different cycles. It is observed that the shape of voltage curves is basically unchanged throughout the entire life span, but they rotate clockwise at a certain point with battery aging. Due to performance degradation, the voltage of an old battery declines faster than that of a new one. And this leads to capacity changes of a battery over its lifetime.

3. Testing Procedures

To study the performance degradation of high-capacity VRLA batteries, a GFM-200 lead acid battery is employed to conduct the cyclic charge-discharge testing. The battery is produced by the Ainuosi-Huada Power System Ltd. (China) and used as backup power supply on the ship. Its nominal capacity is 200 Ah, and the charge and discharge cut-off voltages are 2.35 V and 1.8 V, respectively. According to the constant current and constant voltage (CC-CV) charge and constant current (CC) discharge regimes [7], the testing, which is conducted by the ACCEXP battery test system, followed the steps presented below. The testing was conducted in a closed temperature-regulated chamber at 25 Celsius, which can mimic the average conditions on ships approximately. The temperature changes of the battery were very small and hence were assumed to be equal to the chamber temperature:

(1) Charge the battery with the constant current of 0.1 C until the voltage reaches 2.35 V.

(2) Charge the battery with the constant voltage of 2.35 V until the current drops to 1.2 A.

(3) Let the battery have a rest for 0.5 h.

(4) Discharge the battery with the constant current of 0.1 C until the voltage drops to 1.8 V.

(5) Let the battery have a rest for 0.5 h.

(6) Repeat the above steps until the battery reaches the end-of-life.

During the testing, parameters of interest such as voltage, current, and discharge capacity are monitored and recorded automatically. The discharge voltage curves in different cycles are plotted in Figure 3. As the testing proceeds, the discharge voltage curves become steeper and steeper. As a result, the effective discharge time decreases over cycles number as well as delivered capacity.

4. Capacity Fast Prediction of VRLA Batteries

4.1. Discharge Voltage Modeling. The discharge voltage curve contains abundant information about battery performance and health status, thus establishing an accurate discharge model which can help us predict the usable capacity quickly. As the first phase of voltage (steep drop) is very short, it is generally ignored in the discharge voltage modeling. In phase 2, the voltage drops linearly. When most of the usable capacity is delivered, the voltage starts to drop rapidly in phase 3. According to these characteristics, an empirical equation for the discharge voltage of the lead acid battery is proposed by Rynkiewicz [8].

$$U(t) = k_0 - I \cdot k_1 \cdot t - \frac{k_2}{k_3 - I \cdot t}, \tag{5}$$

where $U(t)$ is the discharge voltage over time, t is the discharge time in hour (h), I is the discharge current in ampere (A), k_0 is a constant for the initial volt (V), k_1 is a constant for the effective resistance in ohm, k_2 captures the concentration of electrolyte, and k_3 represents the final capacity of all active materials.

The voltages in each cycle are fitted to (5), respectively. The voltages in the first 5 minutes (corresponding to the steep drop phase) are removed to improve fitting accuracy. Figure 4 shows changes of each parameter over cycles number. As shown in the plots, the initial voltage (k_0) and effective

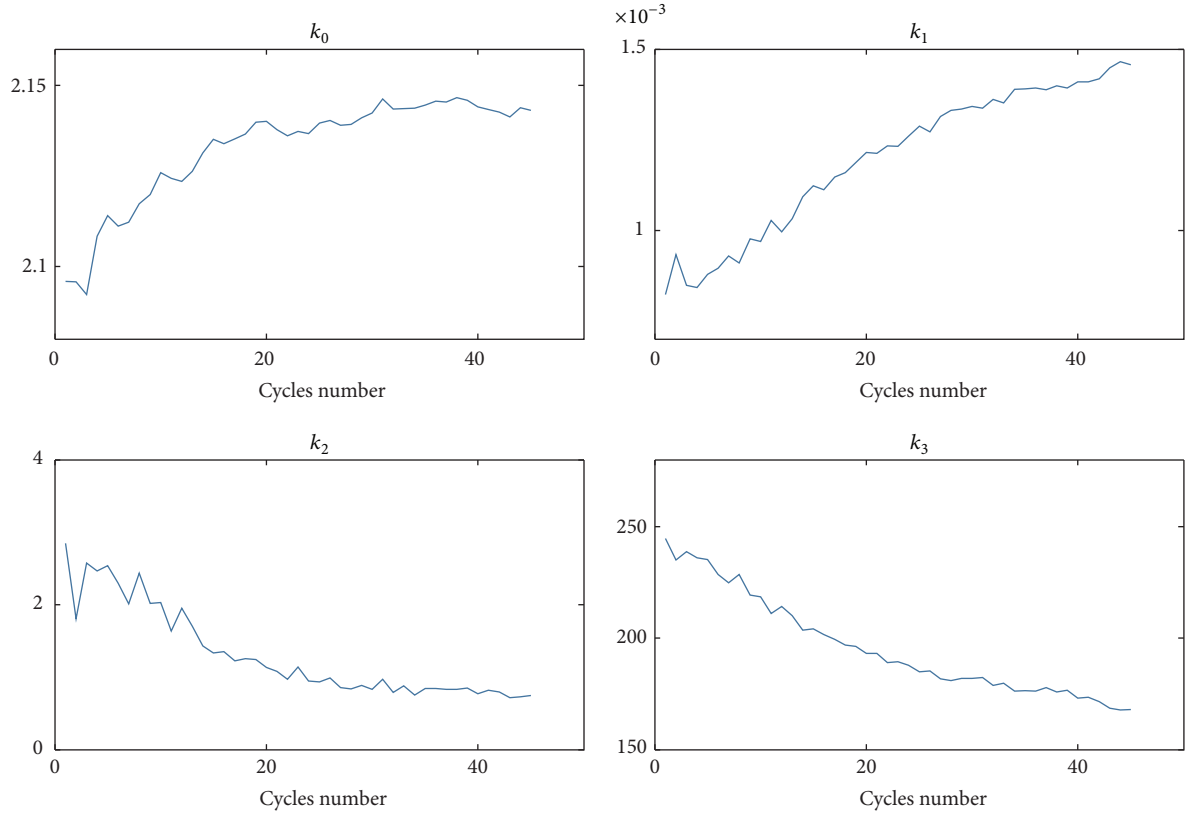

Figure 4: Changes of model parameters in (5).

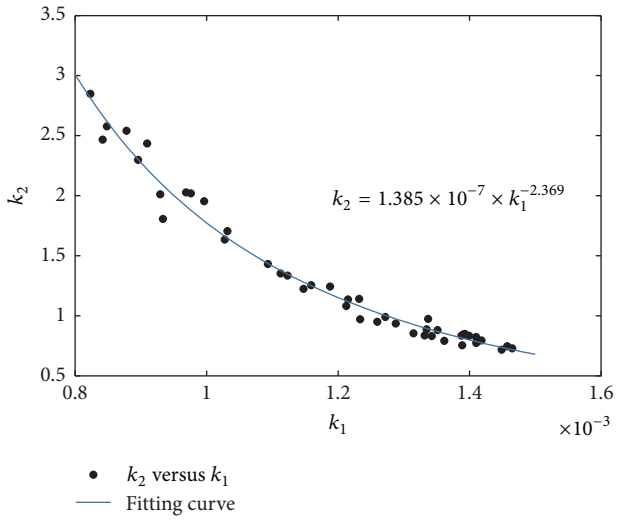

Figure 5: Fitting result of k_2 versus k_1.

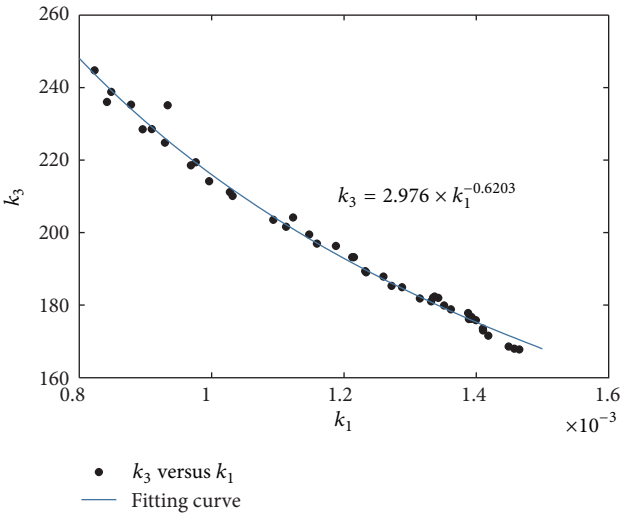

Figure 6: Fitting result of k_3 versus k_1.

resistance (k_1) increase over time, while the concentration of electrolyte (k_2) and final capacity (k_3) decrease. All these phenomena are in line with the performance degradation of lead acid battery.

Furthermore, we find that parameters k_2 and k_3 both strongly correlate with k_1. As Figures 5 and 6 show, the power function is suitable to model their relationships. That is to say, for a given battery, parameters k_2 and k_3 can be estimated by substituting k_1 into the following equation:

$$k_2 = 1.385 \times 10^{-7} \times k_1^{-2.369}$$
$$k_3 = 2.976 \times k_1^{-0.6203}. \quad (6)$$

4.2. Capacity Prediction. Theoretically, battery capacity can be measured by fully discharging it and integrating the discharge current. However, this method is not applicable to high-capacity batteries, since it takes a long time to discharge (at least 10 hours) and shortens battery life seriously owing to the deep discharge. Thus, a fast capacity prediction method for high-capacity VRLA batteries is necessary. According to the aforementioned definition of usable capacity for lead acid battery, it can be calculated by the following equation:

$$C = I \times t_c, \tag{7}$$

where I is the discharge current and t_c is the time it takes when the voltage of a fully charged battery declines to the discharge cut-off voltage.

After obtaining the estimators of k_0, k_1, k_2, and k_3, the fully discharging time t_c can be calculated easily through (5). Then, the issue of capacity fast prediction is converted to the issue of parameter estimation in (5). It is easy to predict k_2 and k_3 by (6), so the remaining issue we should overcome is how to estimate k_0 and k_1 as fast as possible.

In this paper, we aim to predict the usable capacity of a given battery by only discharging it for 3.5 hours instead of 10 hours (the currently shortest fully discharging time). In Figure 3, it is observed that the battery voltage drops linearly in the first 3.5 hours. Thus, a linear equation is employed to fit the voltage during the period; namely,

$$U(t) = a - b \cdot I \cdot t. \tag{8}$$

The estimators of parameters a and b are plotted in Figures 7 and 8. The results reveal that a is in good agreement with k_0, and the linear correlation between b and k_1 is significant. Thus, we can predict k_0 and k_1 by substituting a and b into the following equation:

$$\begin{aligned} k_0 &= a \\ k_1 &= 0.9089 \cdot b - 9.996 \times 10^{-5}. \end{aligned} \tag{9}$$

Now, the procedure of capacity fast prediction can be summarized as follows.

Algorithm 1 (capacity fast prediction).

Step 1. For a given battery, charge it with the normal CC-CV regime until it is fully charged.

Step 2. Discharge it at the constant current of 0.1 C for 3.5 h.

Step 3. Estimate parameters a and b by fitting the voltages obtained in Step 2 with (8).

Step 4. Estimate k_0, k_1, k_2, and k_3 by substituting the estimators of a and b into (9) and (6).

Step 5. Calculate t_c by substituting k_0, k_1, k_2, and k_3 into (5).

Step 6. Predict the usable capacity by substituting t_c into (7).

In the preceding discussion, the partially discharging time is set to be 3.5 hours. To demonstrate that that is a reasonable time, Figure 9 compares the capacity prediction results under different discharging time. In Figure 9, the dotted lines denote the actual capacity measured by the "standard" fully discharging method, and the solid lines are the predicted values by Algorithm 1. The mean relative errors are defined as follows:

$$\text{MRE} = \frac{1}{n} \sum_{i=1}^{n} \frac{\left| C_i^p - C_i^a \right|}{C_i^a} \times 100\%, \tag{10}$$

where C_i^p and C_i^a denote the predicted capacity and actual capacity at the ith cycle and n is the number of cycles.

The MRE under 1.5, 2.5, 3.5, and 4.5 h discharging time are 5.14%, 3.08%, 1.31%, and 1.05%, respectively.

As the length of partially discharging time increases, the prediction accuracy improves. However, when the time exceeds 3.5 hours, the effect of accuracy improvement by

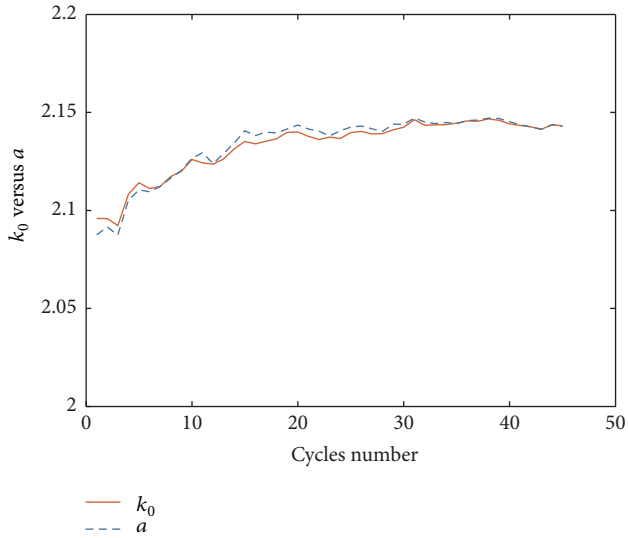

Figure 7: Relationship between k_0 and a.

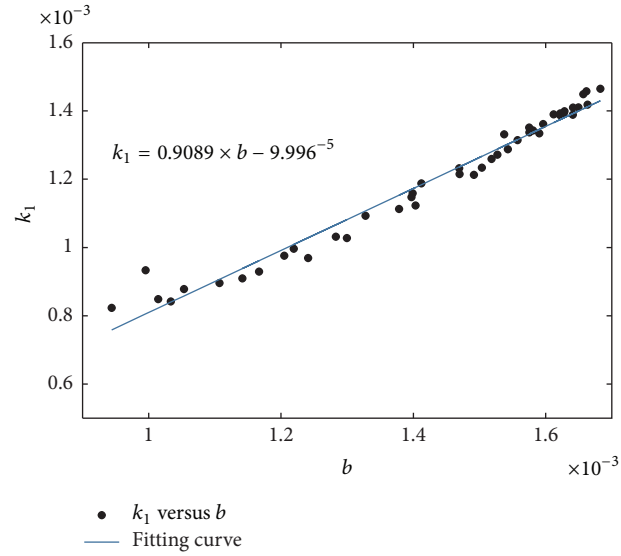

Figure 8: Fitting result of k_1 versus b.

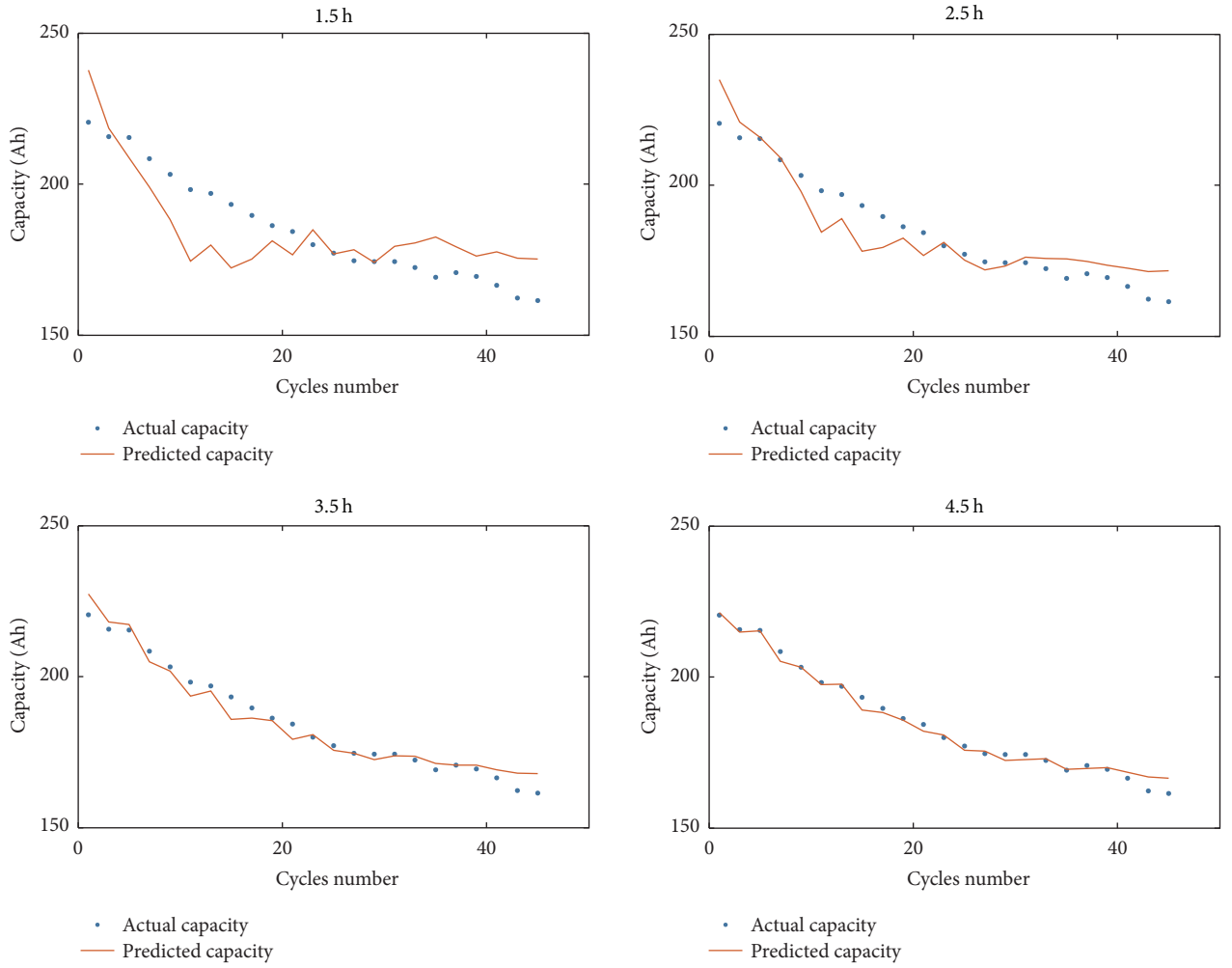

Figure 9: Results of capacity fast prediction under different partially discharging time (GFM-200 battery).

increasing discharging time is no longer remarkable. Thus, we choose 3.5 hours as the partially discharging time in this paper by considering the factors of time and accuracy comprehensively.

To further demonstrate the effectiveness of our method, we use the steps and parameters above to predict the capacity of another VRLA battery GFM-100. The only difference between GFM-200 and GFM-100 is that the latter nominal capacity is 100 Ah. GFM-100 was also tested with the CC-CV charge and CC discharge regimes at 25 Celsius. In the prediction procedure, the partially discharging time is set to be 3.5 hours. Figure 10 compares the actual capacity and predicted values of GFM-100. The MRE of prediction for GFM-100 is 2.71%. It is observed that the prediction results are still accurate except for the first few cycles. The main reason may lie in the fact that the discharge characteristics of different batteries show some heterogeneity as a result of the randomness of materials.

5. RUL Estimation

Recently, engineers have paid more attention to the online safety, risk management, and maintenance decision of equipment in the defense industry [9–11]. RUL estimation plays an important role in the risk management and condition-based maintenance of VRLA batteries for marine backup power use. As discussed above, the usable capacity and stability of a VRLA battery decrease during either storage or operation. Before a battery fails, it must be replaced by a new one to avoid unexpected failures and accidents [12, 13]. The predicted capacity in Section 4 can be used as the degradation feature to infer RUL distributions (RLDs).

5.1. Particle Filtering. Degradation modeling and parameter updating are keys of online RUL estimation. The degradation process of battery capacity can be treated as an underlying random process. With the predicted capacity, an empirical model can be easily established to describe the common degradation characteristics. To capture the online variability of a battery, model parameters used for prediction should be updated once new capacity measurement is available. In order to characterize the dynamic capacity fading, the particle filtering approach is used in this paper to timely update the parameters distribution. Particle filtering is a sequential Bayesian method based on the technique of Monte Carlo simulation [14]. Compared with the Kalman filtering, it can

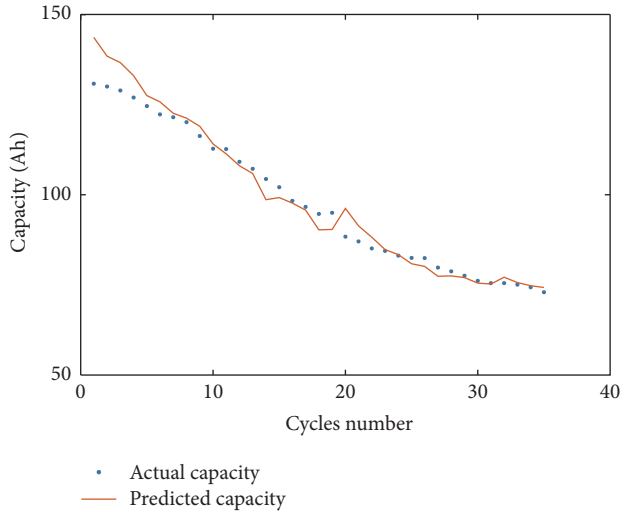

FIGURE 10: Results of capacity fast prediction of GFM-100 battery.

deal with nonlinear model and non-Gaussian noise system. And thus it is widely used in the field of prognostics [15].

In the framework of particle filtering, a state-space model is used to characterize the evolution of degradation feature and model parameters (known as states vector). In the case of VRLA batteries, the degradation feature is battery capacity and the degradation path can be expressed by an exponential function (as Figure 9 shows). Motivated by [16], the parameters are not dynamic and can be regarded as constant between two time points. Thus, the state-space model is as follows.

State Transition Function

$$\begin{aligned} x_i &= \exp\left(-b_i \Delta t\right) x_{i-1} \\ b_i &= b_{i-1} \\ \sigma_i &= \sigma_{i-1}, \end{aligned} \tag{11}$$

Observation Function

$$y_i = x_i + v_i, \tag{12}$$

where $\Delta t = t_i - t_{i-1}$, x_i is the uncontaminated signal (namely, actual capacity) at t_i, y_i is the observation (namely, predicted capacity) including Gaussian noise v_i, b_i is the parameter of the exponential function, and the standard deviation of v_i is σ_i.

A set of particles are generated by the Monte Carlo simulation to estimate the current capacity x_i as well as distributions of parameters b_i and σ_i. Once new observation is available, these particles are resampled to approximately denote the posterior distribution. More details about the theories of particle filtering can be found in [17, 18]. After obtaining the observations $y_1, y_2, \ldots, y_k$ (y_k is the latest observation time), the standard particle filtering for RUL estimation is as follows.

Algorithm 2 (standard particle filtering for RUL estimation).

Step 1 (particles initialization). Due to lack of prior information, N initial particles of the state vector $\{x_0, b_0, \sigma_0\}^p$, $p = 1, 2, \ldots, N$, are sampled from uniform distributions.

For $i = 1 : k$.

Step 2 (particles updating). According to the state transition function (11), update the particles to the next moment; namely,

$$\{x_{i-1}, b_{i-1}, \sigma_{i-1}\}^p \longrightarrow \{x_i, b_i, \sigma_i\}^p. \tag{13}$$

Step 3 (weights calculation). Calculate the weight ω_i^p of each particle, which is proportional to the value of likelihood function given the current observation y_i; namely,

$$\omega_i^p \propto \frac{1}{\sqrt{2\pi}\sigma_i^p} \exp\left\{\frac{1}{2}\left(\frac{y_i - x_i^p}{\sigma_i^p}\right)^2\right\}, \quad p = 1, 2, \ldots, N. \tag{14}$$

Step 4 (particles resampling). Resample particles $\{x_i, b_i, \sigma_i\}^p$ according to weights ω_i^p, $p = 1, 2, \ldots, N$.

Step 5. Repeat Step 2 to Step 4 until $i = k$, and the N particles $\{x_k, b_k, \sigma_k\}^p$ in Step 4 can be used to approximate the posterior distribution of states vector at t_k.

Step 6. Propagate particles using (11), and a threshold level D_f is specified to extrapolate the N pseudo-RLs, denoted as $\{\mathrm{RL}_k^1, \mathrm{RL}_k^2, \ldots, \mathrm{RL}_k^N\}$, which can approximate the actual RLD at t_k.

5.2. Results Analysis. The data used as observations are the fast prediction results of the GFM-200 VRLA battery. For simplicity, the capacity predictions are normalized as follows:

$$y_i = \frac{C_i}{C_1}, \tag{15}$$

where C_i is the predicted capacity in the ith cycle.

In this study, the end-of-life corresponds to the moment when the usable capacity degrades to 80% of the initial value; that is to say, the failure threshold is set to be 0.8. Under the failure criterion, the actual cycle life of GFM-200 battery is 27 cycles.

Updating is conducted every 5 cycles, from the 1st cycle to the EOL. The number of particles is set to be 5000. Figure 11 presents the procedures of RUL estimation at the 15th cycle. The observation at each cycle is marked by a blue dot, and the red line and dotted lines denote the median and 80% confidence intervals of the predicted normalized capacity in the particle filtering, respectively. Results show that the median predictions are very close to the observations after online updating. The histogram in Figure 11 is the

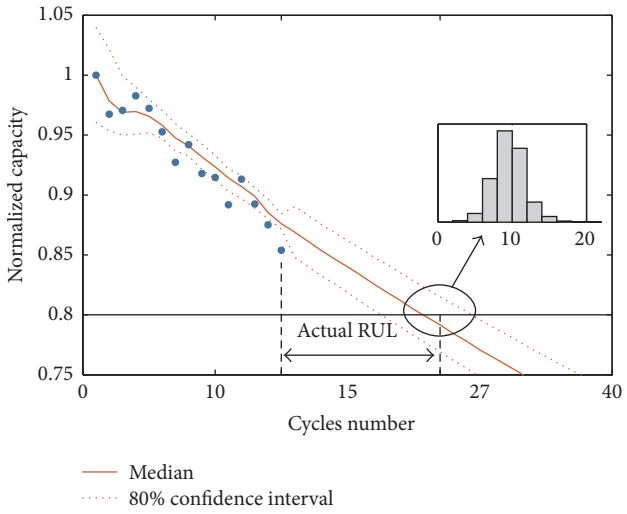

Figure 11: RUL estimation of GFM-200 battery at the 15th cycle.

Table 1: RUL estimation of GFM-200 battery at the 10th, 15th, and 20th cycles.

Current cycle	Actual value	Mean	Median	80% confidence intervals
10	17	20.4	19	[14, 27]
15	12	10.9	11	[8, 14]
20	7	6.7	6	[4, 10]

approximated RLD at the 15th cycle, which matches quite well with the actual RUL (12 cycles). The actual value, mean, median, and 80% confidence intervals of the RUL estimation at the 10th, 15th, and 20th cycles are shown in Table 1. It is clear that the actual RUL falls with the range of 80% confidence intervals, indicating that RUL estimation in this paper is very accurate.

6. Conclusion and Future Work

It is well known that the usable capacity is a key indicator measuring the performance degradation of secondary batteries. In this paper, a RUL estimation framework based on the technique of usable capacity fast prediction is presented for the high-capacity VRLA batteries. The capacity fast prediction approach is conducted using the partially discharging voltages, and the particle filtering method is used to update the capacity degradation model timely. From the experiment results, we observe that the proposed framework can effectively realize VRLA battery capacity prediction as well as RUL estimation. With the advantage of generalization, the approaches in this paper can be easily extended to other types of secondary batteries. In this work, we did not consider the effects of temperature changes on prediction accuracy. In practice, batteries are usually operating under varying temperatures. If necessary, future research may add temperature to the prediction model.

Competing Interests

The authors declare that there is no conflict of interests regarding the publication of this paper.

Acknowledgments

This work is supported by the Chinese National Science Foundation (Grants no. 71271212) and the Natural Science Foundation of Hunan Province (Grants no. 14JJ3009).

References

[1] W. G. Hurley, Y. S. Wong, and W. H. Wölfle, "Self-equalization of cell voltages to prolong the life of VRLA batteries in standby applications," *IEEE Transactions on Industrial Electronics*, vol. 56, no. 6, pp. 2115–2120, 2009.

[2] S. Ken, T. Yuichi, and S. Masashi, "Corrosion of PbCaSn alloy during potential step cycles," *Journal of Power Sources*, vol. 175, no. 1, pp. 604–612, 2008.

[3] Q. Huangpeng, Q. Sun, J. Feng, Z. Q. Pan, and D. Wub, "Cycle life prediction for space nickel hydrogen battery based on accelerated EODV multi-phase model," *Journal of the Electrochemical Society*, vol. 162, no. 4, pp. A658–A666, 2015.

[4] M. Shahriari and M. Farrokhi, "Online state-of-health estimation of VRLA batteries using state of charge," *IEEE Transactions on Industrial Electronics*, vol. 60, no. 1, pp. 191–202, 2013.

[5] M. Einhorn, F. V. Conte, C. Kral, and J. Fleig, "A method for online capacity estimation of lithium ion battery cells using the state of charge and the transferred charge," *IEEE Transactions on Industry Applications*, vol. 48, no. 2, pp. 736–741, 2012.

[6] H. L. Wang and S. M. Cui, "Modeling of the characteristics of charge and discharge of lead-acid battery based on test," *Chinese LABAT Man*, vol. 42, pp. 38–40, 2005.

[7] B. R. Thomas, *Linden's Handbook of Batteries*, McGraw-Hill, New York, NY, USA, 4th edition, 2010.

[8] R. Rynkiewicz, "Discharge and charge modeling of lead acid batteries," in *Proceedings of the 14th annual Applied Power Electronics Conference and Exposition (APEC '99)*, pp. 707–710, IEEE, Dallas, Tex, USA, March 1999.

[9] X. Yu and J. Jiang, "Hybrid fault-tolerant flight control system design against partial actuator failures," *IEEE Transactions on Control Systems Technology*, vol. 20, no. 4, pp. 871–886, 2012.

[10] X. Yu and J. Jiang, "A survey of fault-tolerant controllers based on safety-related issues," *Annual Reviews in Control*, vol. 39, pp. 46–57, 2015.

[11] X. Yu, Y. M. Zhang, and Z. X. Liu, "Fault-tolerant flight control design with explicit consideration of reconfiguration transients," *Journal of Guidance, Control, and Dynamics*, vol. 39, no. 3, pp. 556–563, 2016.

[12] D. H. Liu, H. Wang, Y. Peng, W. Xie, and H. T. Liao, "Satellite lithium-ion battery remaining cycle life prediction with novel indirect health indicator extraction," *Energies*, vol. 6, no. 8, pp. 3654–3668, 2013.

[13] W. L. Burgess, "Valve Regulated Lead Acid battery float service life estimation using a Kalman filter," *Journal of Power Sources*, vol. 191, no. 1, pp. 16–21, 2009.

[14] Y. Liu, B. He, F. Liu, S. Lu, Y. Zhao, and J. Zhao, "Remaining useful life prediction of rolling bearings using PSR, JADE, and extreme learning machine," *Mathematical Problems in Engineering*, vol. 2016, Article ID 8623530, 13 pages, 2016.

[15] M. S. Arulampalam, S. Maskell, N. Gordon, and T. Clapp, "A tutorial on particle filters for online nonlinear/non-Gaussian Bayesian tracking," *IEEE Transactions on Signal Processing*, vol. 50, no. 2, pp. 174–188, 2002.

[16] G. Jin, D. E. Matthews, and Z. Zhou, "A Bayesian framework for on-line degradation assessment and residual life prediction of secondary batteries in spacecraft," *Reliability Engineering and System Safety*, vol. 113, pp. 7–20, 2013.

[17] D. An, J.-H. Choi, and N. H. Kim, "Prognostics 101: a tutorial for particle filter-based prognostics algorithm using Matlab," *Reliability Engineering and System Safety*, vol. 115, pp. 161–169, 2013.

[18] B. Saha, C. C. Quach, and K. Goebel, "Optimizing battery life for electric UAVs using a Bayesian framework," in *Proceedings of the IEEE Aerospace Conference*, pp. 1–7, Dayton, Ohio, USA, March 2012.